Journal of the Optical Society of Korea, Vol. 7, No. 4, December 2003, pp. 216-223

Spatial Resolution Enhancement with Fiber-based Spectral Filtering for Optical Coherence Tomography

EunSeo Choi, Ji-hoon Na, and Byeong Ha Lee*

Department of Information and Communications, Kwangju Institute of Science and Technology, Gwangju 500-712, KOREA

(Received October 5, 2003)

We report a technique that improves the spatial resolution of optical coherence tomography (OCT) by utilizing fiber-based spectral filtering. The proposed technique improves the resolution by filtering out the erbium's characteristic peak from the amplified spontaneous emission (ASE) source spectrum, and reshaping the spectrum to Gaussian-like. We used a long period fiber grating (LPG) and an erbium doped fiber (EDF) absorber for the spectral filtering. An in-house made ASE source as well as a commercial ASE source [ASE-FL7002] was used as the OCT sources to study the proposed technique. The resolution of the OCT based on an in-house made ASE source is enhanced from 200 to 40 μm with an LPG. While, the resolution of the OCT based on a commercial ASE source is enhanced from 25 to 19 μm with the aid of an EDF absorber. However, sidelobes still exist in the interferogram due to imperfect spectral filtering, which limited the resolution. Further enhancement in the spatial resolution of the OCT system using the ASE source is possible with the aid of cascaded LPGs and/or carefully designed EDF absorber.

OCIS codes : 170.0045, 170.3880, 120.3890.

I. INTRODUCTION

Optical coherence tomography (OCT) is considered as a promising candidate for future imaging modality because it allows non-invasive cross-sectional imaging of a microstructure with a high-resolution and a wide dynamic range [1]. *In vivo* and real-time image acquisition capability are the merits of OCT [2]. High-resolution imaging performance up to micrometer level distinguishes itself from other imaging modalities [3,4]. Owing to the need for comprehensive understanding of an unknown sample's complicated microstructure, the enhancement of OCT resolution has been the core of numerous researches.

The spatial resolution of the OCT is mainly determined by the source parameters. The relationship between the resolution and the source parameters can be explained with the coherence length of the source. OCT systems have adapted light sources having low coherence lengths, or broadband light sources, because higher spectral bandwidth provides better resolution in the OCT image. Further reduction in the coherence length of the source will enable visualization of the sub-cellular structures of a living tissue [5].

The techniques used in the development of OCT sources to obtain the high resolution can be classified into three types. The first method is broadband source generation, or supercontinuum generation, using an ultra-short pulse laser and specialty fibers (for example, photonic crystal fiber [6] or tapered fiber). It can produce a source having a high power and a wide bandwidth in the order of 100 nm [7]. Although this method provides the broadband source required for high-resolution OCT, it makes the system expensive and bulky. Further, unstable operation, fluctuations in the emitting power, and the non-Gaussian spectral shape of the supercontinuum source need to be addressed for it to be appropriate for a practical OCT system. The second approach for the realization of the higher resolution is the synthesis of the source spectrum with cascaded light emitting diodes (LEDs) [8]. Each LED has a bandwidth of 20 nm. Thus, cascading several LEDs having closely-spaced center-wavelengths can yield a large bandwidth source with a short coherence length, which is the essential feature of the high-resolution OCT sources. However, the non-Gaussian shape of the spectrum induces large sidelobes, which distorts the fine features in the OCT image. Another major disadvantage of this method is that the obtainable op-

tical power is low compared with that of superluminescent diode (SLD) or amplified spontaneous emission (ASE) source. The last technique uses the spectral tailoring of a given source. In this technique, the non-Gaussian shape of the source spectrum is modified to the Gaussian to improve the resolution of the OCT system. Since the spectral shapes of most available sources are non-Gaussian, sidelobes in the interferogram are inevitable. To remove or reduce the sidelobes, the dispersion control or Fourier component correction method has been developed [9,10]. However, if spectrally tailored sources are used in OCT, there will not be any need for post-processing.

Commonly used OCT sources are SLD, edge-emitting LED (EELED), and ASE sources. Among them, the ASE source is the only fiber-based light source, which is constructed with erbium-doped fiber (EDF) and a 980 nm LD pump. Because it is a fiber-based source, the insertion loss in the source-to-fiber coupling is low, which makes it practical for fiber-based OCT systems and also makes the system compact. Besides, it also has notable features such as a high emitting power and low cost. Further, broadband operation can be achieved by combining differently doped rare-earth fibers. By using an in-house made ASE source, the cost can be reduced while still keeping the advantages of a good source such as high power (few tens mW) and wide bandwidth (>80 nm). Because wide research results for ASE sources are available in the optical communication fields, enhancement of the source property can be done easily. Since the scattering in a tissue is related to the wavelength as λ^{-4}, in principle, the ASE source having the peak around 1530 nm would be preferred to the commercial sources centered around 1300 nm for OCT. However, the spectrum of the ASE source typically has a high and narrow characteristic peak due to the property of the erbium dopant in the EDF. When the ASE source is used as an OCT source, the high and narrow peak in the spectrum reduces the spatial resolution and induces high and wide sidelobes in the interferogram. Despite many advantages of the ASE source, the characteristic peak in the spectrum limits its use as an OCT source. If the high and narrow peak of the ASE source can be reduced by suitable spectral tailoring, it becomes feasible to use the ASE source as an OCT source.

For this reason, we have focused our attention on the spectral tailoring of the ASE source, thus enhancing the resolution of OCT. Since water has large absorption near the center wavelength of the ASE source, we can use the ASE source based OCT for studying the specimens containing low water content such as bones and tooth.

In this paper, we present the simulation results, which indicate the dependency of the OCT spatial resolution on the source parameters. Especially, dependency of the resolution on the bandwidth and the spectral shape of the source will be explained. In the following sections, we discuss the experimental and the simulated results of two different spectral tailoring techniques used to modify the shape of the spectrum to Gaussian-like. In the first technique, a long period fiber grating (LPG) is used for spectral filtering, and the other technique is based on an EDF absorber. We also explain the spectral tailoring capability of the EDF absorber by using a simple energy diagram and the gain-absorption spectrum of erbium. Finally, the OCT image of an onion is presented to demonstrate the enhancement of the resolution.

II. OCT SPATIAL RESOLUTION DETERMINIATION

The resolution of an OCT system is limited by various system parameters such as source characteristics, mechanical stability, and noises in electronic signal processing. In OCT, the spatial resolution is strongly dependent on the source parameters such as the center wavelength, the bandwidth and the shape of the spectrum. For the ideal OCT source with Gaussian spectrum and no dispersion, the spatial resolution of the OCT is given by [11,12]

$$\Delta x = \frac{2\ln 2}{\pi}\frac{\lambda_c^2}{\Delta\lambda} \cong 0.44\frac{\lambda_c^2}{\Delta\lambda} \qquad (1)$$

where Δx, λ_c and $\Delta\lambda$ are the spatial resolution, the center wavelength and the full width at half maximum (FWHM) bandwidth of the source.

Since the center wavelengths are similar in most available OCT sources, the variable source parameters affecting the resolution are the bandwidth and the spectral shape. From the above formula, the relation between the resolution and the bandwidth can be easily understood: the spatial resolution (Δx) is inversely proportional to the bandwidth of the source ($\Delta\lambda$). It can be also interpreted as the source having larger bandwidth provides the higher resolution in OCT. The equation can be easily derived from the autocorrelation function of the source, which is related to the Fourier transformation of the power spectral density of the source [13].

Fig. 1 shows the dependency of the resolution on the bandwidth and the spectral shape of the source. In the simulations, we used Gaussian and flat-top shapes to investigate the effect of the spectral shape on the resolution. For both shapes, the same center wavelength, λ_c = 1550 nm, was used and bandwidths $\Delta\lambda$ ranging from 30 - 200 nm were used to study the effect of the bandwidth on the resolution. Figs. 1(a) and (b)

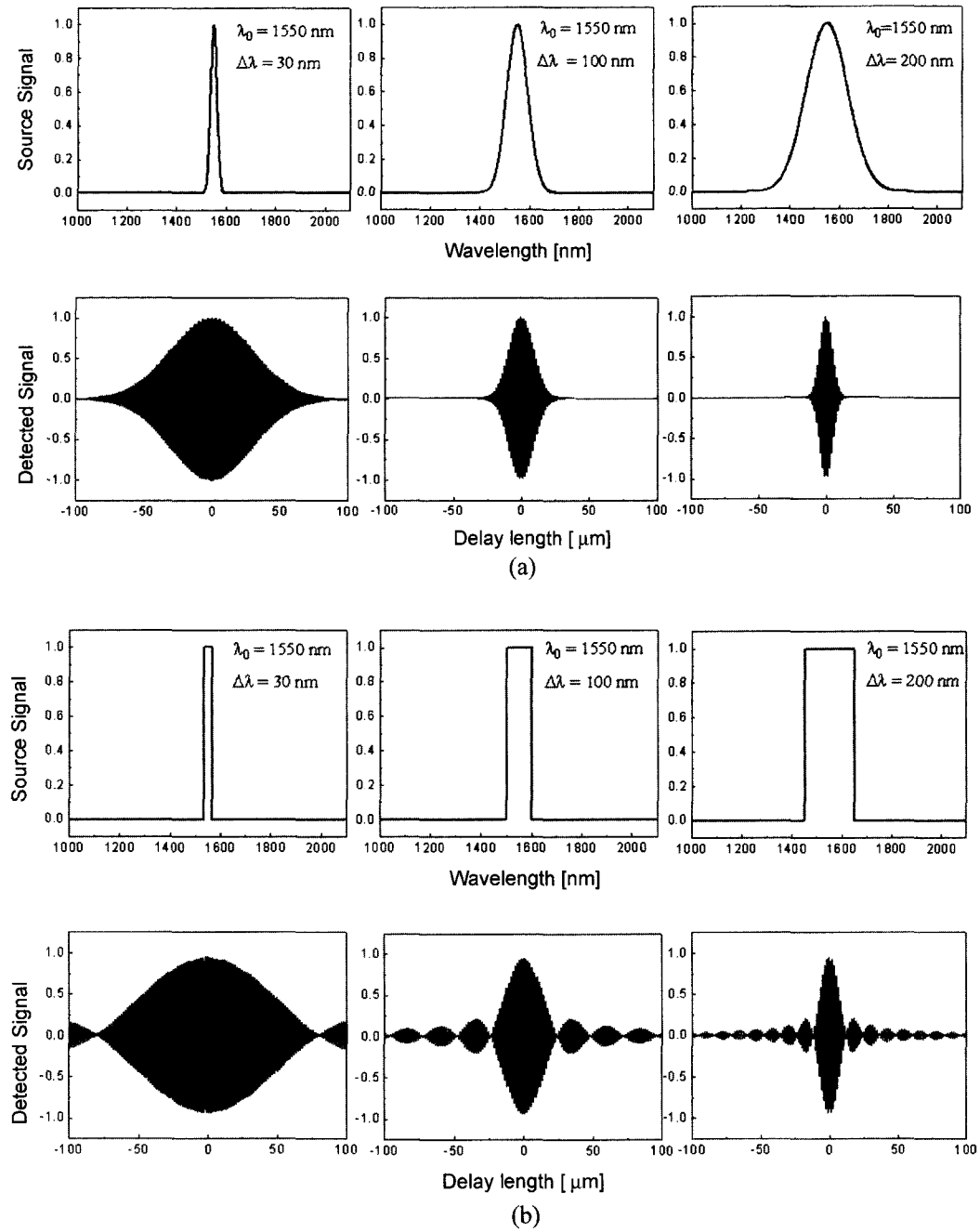

FIG. 1. Resolution dependency on source spectral shape and bandwidth. (a) is for the Gaussian shaped source and (b) is for the flat-top shaped source.

show the simulation results of the resolution for Gaussian and flat-top spectral shapes. In both cases, the resolution increases with the bandwidth but the striking difference is that the shape of the envelope of the interferogram for the Gaussian spectrum remains Gaussian and does not have any sidelobes or spurious patterns which degrade the resolution. The sidelobes in the interferogram degrade the resolution by forming ghost structures in the image. Further, as mentioned, Eq. (1) is applicable only for ideal Gaussian-shaped sources. Thus Eq. (1) cannot be employed to predict the resolution as most commercially available sources are non-Gaussian. Hence Gaussian sources with broad bandwidths are suitable for OCT.

To appreciate the effect of the spectral shape on the formation of the sidelobes in the interferogram, we

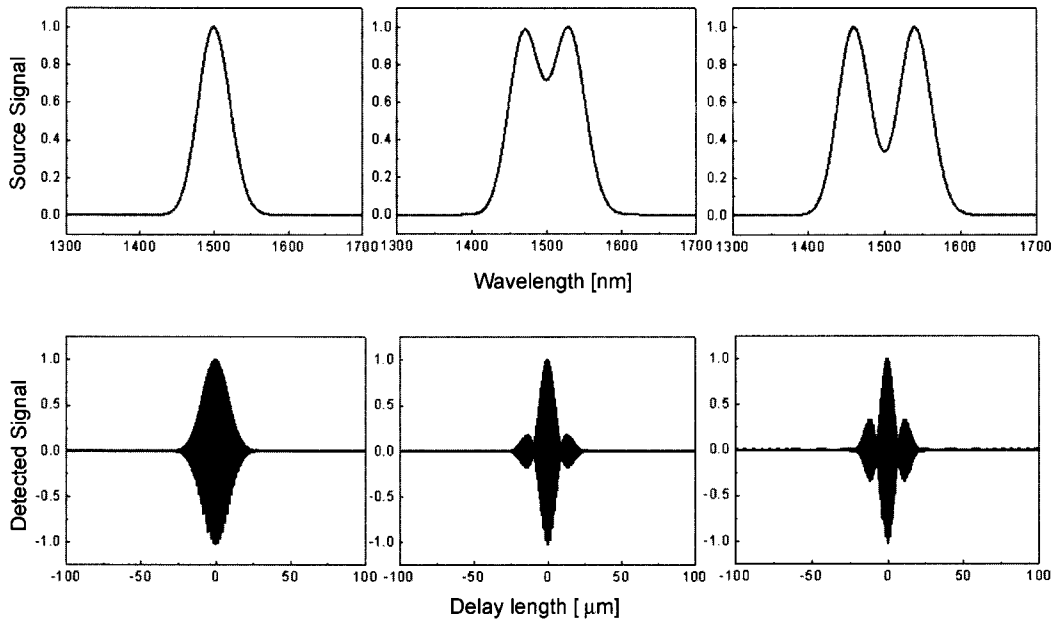

FIG. 2. Sidelobes generation according to the source spectral shape distortion from the Gaussian shape

observed the sidelobes as the shape of the source is distorted from the ideal Gaussian case. We used two identical Gaussian sources ($\lambda_c = 1550$ nm, $\Delta\lambda = 50$ nm) to simulate the over-all shape of the source. By adding these two sources appropriately, we could obtain the over-all source shape, which could be an ideal Gaussian or non-Gaussian shape. Interferograms due to simple source shapes such as Gaussian and flat-top can be predicted by considering the Fourier transformation relation between the source power spectral density and the interferogram. However for the general spectral shapes, expectation of interferogram is not so easy. For this reason, the simulation with the over-all shape was done. Using the results of the simulation, we could appreciate the general trend in the interferogram change. Adding two or more several Gaussian sources happens in cascading LEDs and SLDs.

The results of the simulation are shown in Fig. 2, which clearly show that well-distinguished peaks in the source spectrum induce large sidelobes around the main peak. Since the ghost image due to the sidelobes severely hampers the imaging performance of the OCT systems in clinical applications, a suitable spectral tailoring technique is required to tailor the source spectrum into Gaussian.

III. FIBER-BASED SPECTRAL TAILORING

Spectral filtering process is required for obtaining an enhanced resolution and well-suppressed sidelobes from a non-Gaussian source. In the fiber-based OCT system, spectral shape modification using fiber-based devices is effective in tailoring the source spectrum. Moreover, the fiber-based system is preferred to a bulk-optics system because of compactness and alignment-free characteristics. Therefore, we used fiber-based spectral tailoring technique with an LPG as a band rejection filter and an EDF as a wavelength-dependent power absorber for spectral filtering of the ASE source.

An LPG, which acts as a band-rejection filter, is well known as a gain-flattening filter in optical communication systems. The LPG is fabricated by UV-irradiating the fiber through an amplitude mask with a specific period. The irradiated UV dose and the period of the mask determine the spectrum of the grating. The center wavelength, the bandwidth, and the depth of the grating can be controlled by adjusting the fabrication conditions [14]. The rejection spectrum of the LPG can be adjusted for proper spectral tailoring of the source spectrum.

Various loss mechanisms may be associated with degradation of signals in the optical communication systems. In-line repeaters and amplifiers are used to compensate the power losses in long-haul communication systems. An all-fiber amplifier based on EDF was a major driving force for the development of optical communication networks. The EDF pumped by a 980 nm LD can provide in-line amplification in the optical communication window. However, it behaves as an absorber in the same bandwidth in the absence of the pump. We exploited the absorption property of the EDF to use it for spectral filtering. The principle

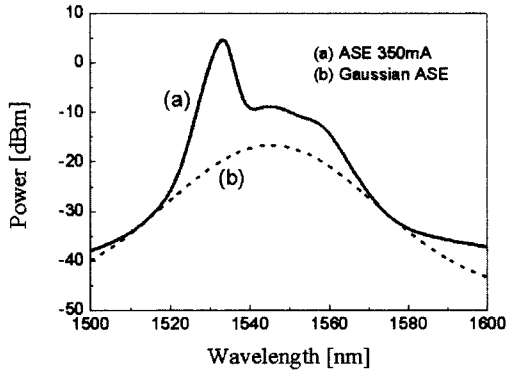

FIG. 3. In-house made and ideal ASE source shape. (a) represents prepared ASE source shape before tailoring and (b) depicts ideally reshaped ASE source.

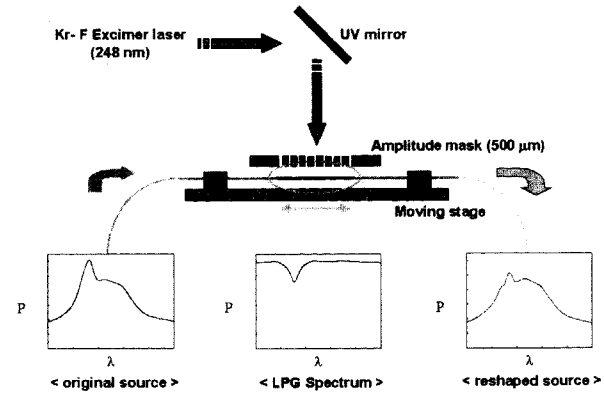

FIG. 5. LPG-assisted spectral tailoring setup and spectral change of the source when an LPG is inserted.

of the spectral filtering using an LPG and the EDF absorber is the same. We essentially utilize them to either reject or absorb in a particular part or band of the spectrum and hence modify the shape of the spectrum to Gaussian and enhance the spatial resolution of OCT.

1. RESOLUTION ENHANCEMENT WITH LONG-PERIOD FIBER GRATING

An in-house made ASE source was constructed with a ~20 m long EDF and a 980 nm pump LD (Max. current is 350 mA). The spectrum of the source is poor compared with the commercial product. The spectrum has a strong and narrow characteristic ASE peak due to the erbium dopant. In Fig. 3, the spectrum of the unprocessed ASE source (a) is compared with the ideal Gaussian spectrum (b) assuming a perfect spectral tailoring. Fig. 4 shows the simulation results, which indicate the enhancement of the resolution after spectral tailoring. The resolution for the perfect spectral filtering case is 40 μm.

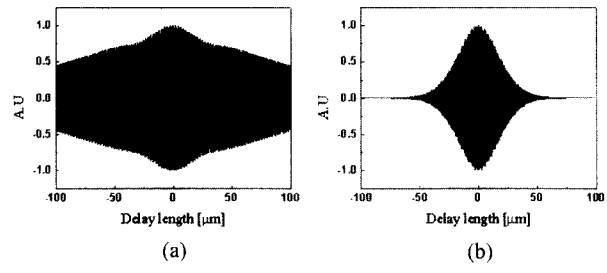

FIG. 4. Simulated interferogram results for source shape in Fig. 3. Expected resolutions are 200 m before tailoring (a) and 40 m after perfect processing (b), respectively.

For the LPG-based spectral filtering, the LPG is connected to the unprocessed ASE source output. In fabrication of the LPG, the scanning method was used for uniform index modulation over the entire grating length. The length and the period of the mask used in fabricating the LPG were 20 mm and 500 μm, respectively. HE_{14} mode was chosen for proper spectral specification. The center wavelength and the depth of the LPG spectrum were adjusted to 1530 nm and 15 dB, respectively. Fig. 5 depicts the setup for the LPG fabrication along with the LPG spectrum and the spectrum of the ASE source before and after the spectral tailoring. By controlling the dose of UV, the spectrum of the LPG was matched with the spectrum of the ASE source for proper spectral tailoring.

Fig. 6 shows the change in the spectrum and the interferogram of the ASE source when the source shape

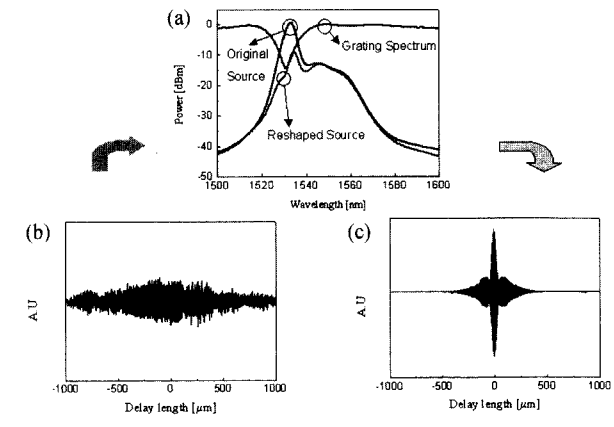

FIG. 6. Resolution enhancement when the spectral tailoring was done by a single LPG. (a) shows the change in spectrum with spectral tailoring and the LPG spectrum used for tailoring. The interferogram of (b) from the original source was dramatically changed into that of (c) after spectral tailoring with an LPG.

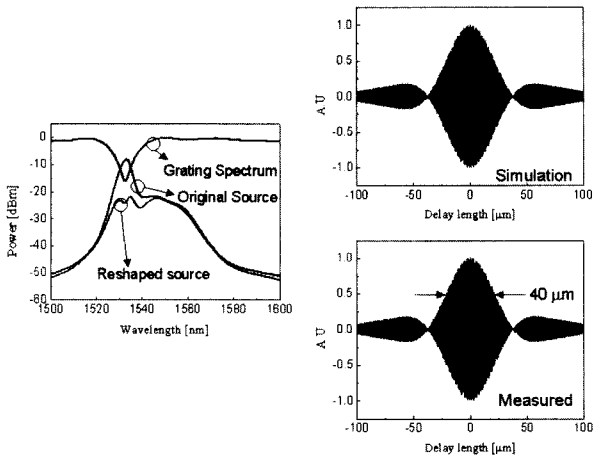

FIG. 7. Resolution enhancement up to 40 m with suppressed sidelobes. The measured results are well matched with the simulated expectation.

was tailored with a single LPG. In the experimental setup, a gold-coated mirror(reflectivity > 95 %) was placed in the sample arm as a perfect reflector. The detailed experimental setup was described in ref. [15]. The experiments have suggested very exciting results. Before the spectral tailoring, the actual spatial resolution in the interferogram was not well defined because of the widely broadened interference pattern all over the delay length, which originated from the strong and distinct peak in the spectrum of the in-house made ASE source. The bandwidth of the peak was less than 5 nm. Using the previous results of Fig. 4(a), we can predict about a 200 μm spatial resolution, which is well matched with the experiment result. However, after filtering with an LPG, the resolution of the ASE source is dramatically improved as shown in Fig. 6(c). By adjusting the LPG fabrication conditions, a more enhanced interferogram was obtained as shown in Fig. 7 and the spatial resolution was enhanced to about 40 μm. This value is matched well with the calculated resolution that is acquired from an ideally tailored Gaussian spectrum. The result means that appreciable resolution enhancement can be achieved by using only a single LPG for spectral tailoring.

But unfortunately, the spectral tailoring with a single LPG has revealed some limitations. Though the resolution was the same as that of the ideal Gaussian source, the non-Gaussian shape of the tailored spectrum has led to the symmetric sidelobes around the main central peak. As shown in Fig. 7, the tailored ASE spectrum is not smooth and far from the ideal Gaussian shape. The sidelobes can be removed only when the shape of the spectrum becomes to Gaussian, which can be obtained by cascading several LPGs.

2. RESOLUTION ENHANCEMENT WITH ERBIUM DOPED FIBER

Usually EDF is used for making a fiber amplifier. However, in the experiment, the absorbing function of the EDF is used instead of the amplification property by removing the pumping source. Fig. 8 shows the energy diagrams of Er and the characteristic absorption and emission trends. The energy levels are largely divided into three bands as shown in the Fig. 8(a). Two pumping levels at 980 nm and 1480 nm wavelengths are available for population inversion. Population inversion by an external pump is followed by relaxation to the ground state with light emissions from 1520 to 1610 nm. Fig. 8(b) shows the gain and absorption characteristics of the EDF [16]. The gain and absorption trends depend on the pumping power. The figure clearly shows that the absorption valley and the gain peak match with each other. ASE sources based on rare-earth doped fiber such as Er will show similar trends. Thus, an EDF can be used as an absorber in the EDF spectral change. Using this property, the high gain peak of the ASE source can be removed with an EDF absorber.

To study the spectral filtering capability of the EDF, we used a commercially available ASE source (Thorlabs. Inc., ASE-FL7002). Compared with the ASE source used in the LPG tailoring experiment, this source has a higher power and a wider bandwidth. Similar to the in-house made ASE source, it has the characteristic peak, although smaller. However the position of the peak is shifted to ~1560 nm wavelength because cascaded rare-earth fibers doped with different doping materials were employed in the

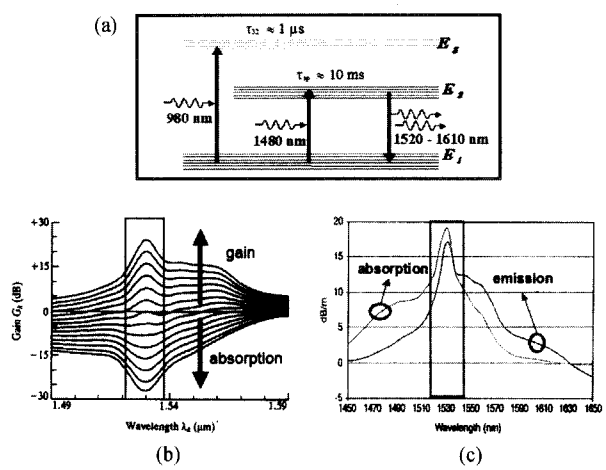

FIG. 8. Spectral tailoring with an EDF absorber. (a) explains energy diagram of erbium and (b) shows gain and absorption trends depend on pumping power. (c) presents similarity between absorption and emission spectrum in the specific window(bold box).

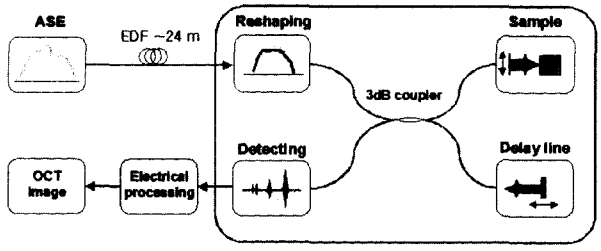

FIG. 9. Spectral tailoring setup with an EDF absorber. EDF is used for absorber without pumping power.

commercial ASE source to obtain larger bandwidth. The EDF absorber could tailor a wider bandwidth of the ASE source compared with the result of the LPG-assisted tailoring. The difference is due to the small variation in the peak position and the similar spectral shapes in the emission and the absorption of the ASE source as shown in Fig. 8(c). For the spectral tailoring with EDF absorber, a ~24 m long EDF was used. Fig. 9 shows the experiment scheme.

The spatial resolution and the optical power before the spectral filtering were measured to be ~25 μm and ~20 mW, respectively. Fig. 10(a) shows the spectral change induced by the EDF absorber. Without spectral tailoring, broad sidelobes were observed in the measured interferogram which overlapped with the main lobe as shown in Fig. 10(b). After the spectral tailoring, the sidelobes were reduced and also became distinguishable from the main lobe enhancing the resolution up to 19 μm although the spectral tailoring has reduced the power by ~5 mW as shown in Fig. 10(a). The original sidelobes spanning up to ~70 μm of the scanning length was reduced and distinguished

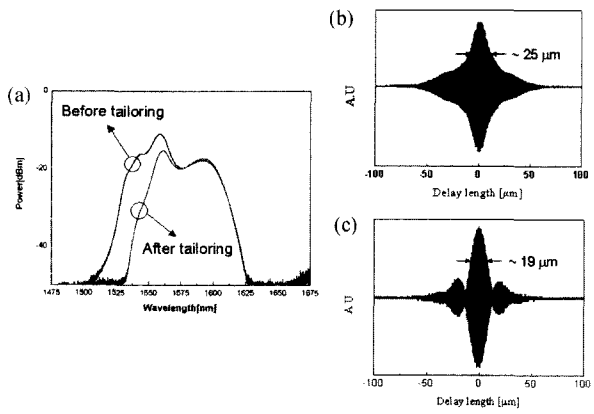

FIG. 10. Spectral tailoring effect of an EDF absorber in the spectrum and interferogram. (a) explains spectrum modification due to wavelength-dependent absorbing function of an EDF. (b) shows the interferogram before tailoring and (c) presents the improved result with the improved resolution and suppressed sidelobes after tailoring.

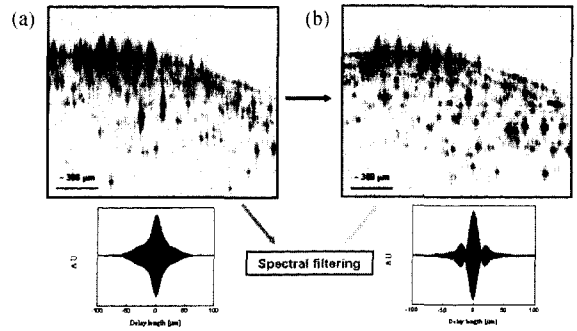

FIG. 11. OCT image enhancement of onion sample when the EDF absorber was applied. (a) and (b) show the OCT image before and after spectral filtering, respectively. Wide sidelobes was removed therefore cells buried in the sidelobes could be distinguished.

from the main peak. However, due to imperfect spectral tailoring and non-Gaussian shape, sidelobes still exist as shown in Fig. 10(c).

The cross sectional images of an onion taken by the OCT using ASE source without and with spectral tailoring are shown in Figs. 11(a) and (b). The dimensions of both images were 460 × 380 pixels and the transverse resolution was 5 μm. After tailoring with the EDF absorber, each cell structure was distinguishable. Because the layers buried by the large original sidelobes were unveiled by the reduction of the sidelobes, the image (b) was rather clearer than the image (a). The experimental results show the potential of the EDF absorber for spectral tailoring to enhance the spatial resolution of OCT. In that sense, we can see that the tailoring has improved the onion imaging a little bit. Precise control of the adjustable parameters such as the length of the EDF and the doping concentration in the fiber fabrication process, can improve the OCT resolution further.

IV. CONCLUSION

We reported fiber-based novel techniques that enhance the OCT resolution. The techniques spectrally tailored in the light source by using a long period fiber grating (LPG) and a piece of erbium doped fiber (EDF). The simulations have shown the dependency of spatial resolution on the source parameters, mainly the spectral shape and the bandwidth. Gaussian and flat-top spectral shapes were used in the simulation to study the dependency of the resolution on the shape of the spectrum. Bandwidths from 30 to 200 nm were used to study the dependency on the bandwidth.

The results showed that a non-Gaussian spectrum produces sidelobes in the interferogram.

Fiber-based spectral filtering can increase the feasibility of ASE light sources for the OCT sources, which have the advantages of high power, large bandwidth and longer central wavelength. We could improve the resolution by removing the characteristic ASE peak in the spectrum, which is the main cause for poor resolution. Using a single LPG we could enhance the resolution up to 40 μm (by 5 times), which was close to the ideal resolution obtainable from a perfect Gaussian source. Using the EDF absorber, we could achieve a resolution of 19 μm. In both experiments, the resolution enhancement was obtained by essentially removing the characteristic ASE peak. Even after spectral filtering, sidelobes still exist in the interferogram due to incomplete spectral filtering. We can completely remove the sidelobes by using cascaded LPGs with well-controlled parameters and/or well-designed EDF absorbers to further enhance the resolution. The proposed fiber-based spectral filtering techniques enable the use of ASE sources in fiber-based OCT systems seeking high resolution.

ACKNOWLEDGEMENT

This work was partially supported by the Korea Science and Engineering Foundation (KOSEF) through Ultra-fast Fiber Optic Networks Research Center at Kwangju Institute of Science and Technology (K-JIST), by the Korean Ministry of Education (MOE) through the Brain Korea 21 Program, and the Ministry of Commerce, Industry and Energy (MOCIE) through the industrial base funding projects.

*Corresponding author : leebh@kjist.ac.kr.

REFERENCES

[1] D. Huang, E. A. Swanson, C. P. Lin, J. S. Schuman, W. G. Stinson, W. Chang, M. R. Hee, T. Flotte, K. Gregory, C. A. Puliafito, and J. G. Fujimoto, "Optical coherence tomography", *Science*, vol. 254, pp. 1178-1181, 1991.

[2] G. J. Tearney, B. E. Bouma, S. A. Boppart, B. Golubovic, E. A. Swanson, and J. G. Fujimoto, "Rapid acquisition of in vivo biological Images using optical coherence tomography," *Opt. Lett.*, vol. 21, no. 17, pp. 1408-1410, 1996.

[3] B. Bouma, G. J. Tearney, S. A. Boppart, M. R. Hee, M. E. Brezinski, and J. G. Fujimoto, "High resolution optical coherence tomographic imaging using a modelocked Ti:Al2O3 laser source," *Opt. Lett.*, vol. 20, no. 1, pp. 1-3, 1995.

[4] W. Drexler, U. Morger, F. X. Kartner, C. Pitris, S. A. Boppart, X. D. Li, E. P. Ippen, and J. G. Fujimoto, "In vivo ultrahigh-resolution optical coherence tomography," *Opt. Lett.*, vol. 24, no.17, pp. 1221-1223, 1999.

[5] B. Povazay, K. Bizheva, A. Unterhuber, B. Hermann, H. Sattmann, A. F. Fercher, W. Drexler, A. Apolonski, W. J. Wadsworth, J. C. Knight, P. St. J. Russell, M. Vetterlein, E. Scherzer, "Submicrometer axial resolution optical coherence tomography," *Opt. Lett.*, vol. 27, no. 20, pp. 1800-1802, 2002.

[6] J. Kim, H. K. Kim, U.-C. Paek, B. H. Lee, and J. B. Eom, "The Fabrication of the Photonic Crystal Fiber and its Properties Measurement," *J. Opt. Soc. Kor.*, vol. 7, no. 2, pp. 150-155, 2003.

[7] I. Hartl, X. D. Li, C. Chudoba, R. K. Ghanta, T. H. Ko, J. G. Fujimoto, J. K. Ranka, R. S. Windeler , "Ultrahigh-resolution optical coherence tomography using continuum generation in an air silica microstructure optical fiber," *Opt. Lett.*, vol. 26, no. 9, pp. 608-610, 2001.

[8] Y. Zhang, M. Sato, and N. Tanno, "Resolution improvement in optical coherence tomography by optical synthesis of light-emitting diodes," *Opt. Lett.*, Vol. 26, no. 4, pp. 205-207, 2001.

[9] R. Tripathi, N. Nassif, J. S. Nelson, B. H. Park and J. F. de Boer, "Spectral shaping for non-Gaussian source spectra in optical coherence tomography," *Opt. Lett.*, vol. 27, no. 6, pp. 406-408, 2002.

[10] E. D. J. Smith, S. C. Moore, N. Wada, W. Chujo, and D. D. Sampson, "Spectral Domain Interferometry for OCDR Using Non-Gaussian Broad-Band Sources," *IEEE Photon. Technol. Lett.*, vol. 13, no. 1, pp. 64-66, 2001.

[11] E. A. Swanson, D. Huang, M. R. Hee, J. G. Fujimoto, C. P. Lin, and C. A. Puliafito, "High speed optical coherence domain reflectometry," *Opt. Lett.*, vol. 17, no. 3, pp. 151-153, 1992.

[12] J. A. Izatt, M. D. Kulkarni, H. Wang, K. Kobayashi, and M. V. Sivak, Jr, "Optical Coherence Tomography and Microscopy in Gastrointestinal Tissues," *IEEE J. Sel. Top. Quantum Electron.*, vol. 2, no. 4, pp. 1017-1028, 1996.

[13] B. E. A. Saleh and M. C. Teich, *Fundamentals of photonics* (John Wiley & Sons. Inc, New York, 1991).

[14] R. Kashyap, *Fiber Bragg Gratings*, (Acamedic Press, New York, 1999).

[15] E. Choi, Y.-J., C. Lee, J. Na, C. Lee, and B. Ha Lee, "OCT Premier in Korea," in *Asian Symposium on Biomedical Optics and Photomedicine 2002*, TB2-2, pp. 142-143, 2002.

[16] E. Desurvire, *Erbium-Doped Fiber Amplifiers: Principles and Applications* (John Wiley & Sons, Inc., New York, 1994).